Nonlocality and discrete cellular methods in optics

Wijers, C.M.J.; de Boeij, P.L.

Published in:
Physica B: Condensed Matter

DOI:
10.1016/S0921-4526(01)00616-0

Publication date:
2001

ELSEVIER

Physica B 305 (2001) 220–232

PHYSICA B

www.elsevier.com/locate/physb

Nonlocality and discrete cellular methods in optics

C.M.J. Wijers[a,*], P.L. de Boeij[b]

[a] *Faculty of Applied Physics, Computational Optics, University of Twente, P.O. Box 217, 7500 AE Enschede, The Netherlands*
[b] *Theoretical Chemistry, Materials Science Centre, Rijksuniversiteit Groningen, Nijenborgh 4, 9747 AG Groningen, The Netherlands*

Received 10 May 2001; accepted 30 May 2001

Abstract

A subdivision of space into discrete cells underlies the traditional discrete dipole model. This model presumes that only nonlocal electric interactions between cells govern the electromagnetic response of a condensed matter system. Apart from the case of simple dielectrics, this is not realistic. Cells can also influence each other directly through the wave functions, when those extend across cell boundaries. In general, such nonlocal quantum mechanical interaction requires the use of nonlocal polarizabilities. In this paper it is shown how existing discrete dipole descriptions for clusters, slabs and (semi)-infinite systems have to be altered to incorporate the effects of nonlocal polarizabilities. The modified method is called discrete cellular method.

Keywords: Nonlocality; Optics; Quantum induction; Reflectance anisotropy; GaAs (1 1 0)

1. Introduction

The introductory parts of a textbook like Born and Wolf [1] show that optics can be started either from a dielectric susceptibility or from an "atomic" kind of modeling. The first approach represents mathematically a continuum description and the second a discrete one. Born calls the building blocks of the discrete modeling "atoms" or "molecules". Necessarily, such "atoms" or "molecules" have to occupy a well defined region of space. Such regions or cells can be defined generally as (simply connected) subvolumes, even without the association to "atoms" or "molecules". The cells should be disjunct. Concepts like polarizability, dipole strength or local field are inherently connected to such cellular subdivision. For the homogeneous bulk the relationship between the discrete and continuum descriptions has been formalized into the Lorentz–Lorenz expression. Systems being inherently inhomogeneous, like surfaces, escape from the basic suppositions underlying the derivation of the Lorentz–Lorenz expression and their optical behavior needs different treatment.

When the cells can be polarized independent of their environment, we have the case covered by traditional discrete dipole theory. In principle, a discrete dipole description can be used for any system where this independency holds. This can be done directly for finite systems (clusters). When the optical system is of infinite (bulk) or semi-infinite (surface) dimensions, treatment is only possible when translational symmetry can be used. This kind of symmetry requires a crystalline configuration of cells. Discrete dipole descriptions for both

*Corresponding author. Tel.: +31-53-489-3107; fax: +31-53-489-2910.

E-mail address: c.m.j.wijers@tn.utwente.nl (C.M.J. Wijers).

0921-4526/01/$ -see front matter
PII: S0921-4526(01)00616-0

bulk and surface types of crystalline configurations have been treated extensively in the literature [2–12]. The issue of this paper is how these descriptions will change if we refrain from the requirement of independently polarizable cells.

The only possible physical meaning of being dependent is that the polarization of a cell influences also the polarization of other cells. Why this occurs can be elucidated in a number of ways. The simplest and also most transparent way to make this influence clear is by having a look at the behavior of the wave function. We pointed out that because of the discrete description itself, space has to be subdivided into cells. Then, in general, the wave function will exist in more than one cell only and it has to be anticipated that cell boundaries will intersect the wave function. A change in the state of polarization of a cell is only possible when the wave function inside that particular cell changes simultaneously. If that particular wave function happens to intersect the cell boundary, this same wave function will change in neighboring cells too. This is inevitable, since the wave function is continuous and differentiable, also at the cell boundary. So the neighboring cell will change its state of polarization as well. We will call this influence quantum induction. The only way to account for quantum induction from an electromagnetic point of view is by making use of a nonlocal polarizability.

Although the possibility of a nonlocal polarizability can be made clear using very basic arguments, there are only very few references in the literature [13] about its possible use within a discrete description. If the wave functions of the system stay entirely within the cells, there is no quantum induction and the familiar description using local polarizabilities can be used. Then the system obeys a classical discrete dipole description. When these effects cannot be neglected we have to use nonlocal polarizabilities. If we mention "nonlocal" in this paper without further details, we will mean nonlocal in the quantum mechanical sense. How the nonlocal cellular polarizabilities have to be obtained will not be given in this paper, but will be published elsewhere [14,15]. Here, we will only present how an in-origin discrete dipole method has to be modified to take into account nonlocal polarizabilities. The resulting method will be called discrete cellular method (DCM).

2. Nonlocal induction

The DCM treats the electromagnetic fields the same way as the discrete dipole method. The continuity equation enables charges and currents to be represented by a continuum polarization field **P**. The Lorentz gauge enables the use of the Hertz potential field **Z** [16]. For the continuum case both fields are related by

$$\mathbf{Z}(\mathbf{r}) = \frac{1}{4\pi\varepsilon_0}\int \mathrm{d}\mathbf{r}'\,\frac{\mathrm{e}^{\mathrm{i}k(\mathbf{r}-\mathbf{r}')}}{|\mathbf{r}-\mathbf{r}'|}\mathbf{P}(\mathbf{r}') \tag{1}$$

for a driving field of frequency $\omega = ck$. The corresponding electric fields **E** are derived from the Hertz potential through

$$\mathbf{E}(\mathbf{r}) = \nabla\nabla^{\mathrm{T}}\mathbf{Z}(\mathbf{r}) - \frac{1}{c^2}\frac{\partial^2\mathbf{Z}(\mathbf{r})}{\partial t^2}, \tag{2}$$

where we refer for the upper T convention to Ref. [11]. A product of two vectors without upper T, will be the inner product by default. The continuum equations yield upon discretization the discrete dipole and discrete cellular descriptions. A subdivision of space into N subvolumes V_i, discretizes Eq. (1) and yields the approximate description

$$\mathbf{Z}(\mathbf{r}) = \frac{1}{4\pi\varepsilon_0}\sum_{j=1}^{N}\frac{\mathrm{e}^{\mathrm{i}k|\mathbf{r}-\mathbf{r}_j|}}{|\mathbf{r}-\mathbf{r}_j|}\mathbf{p}_j,$$

$$\mathbf{p}_j = \int_{V_j}\mathrm{d}\mathbf{r}'\mathbf{P}(\mathbf{r}'). \tag{3}$$

The $\mathbf{p}_j$ are the *dipole strengths* of the system. The issue of how to choose the cell coordinate $\mathbf{r}_j$ and how to define the cell boundaries as a general problem, will not be treated here. The DCM is intended to use the one-atom one-dipole assignment. In the past, a similar assignment in the discrete dipole treatment has turned out to be problematic [17]. We will use cells containing one atom and having the nuclear coordinate as cell coordinate. The cells are of Voronoi type, constructed from the perpendicular bisecting planes of

the vectors connecting neighboring cell coordinates.

Eqs. (2) and (3) give the electromagnetic fields within a discrete dipole or discrete cellular kind of description, including their nonlocal behavior. The discrete dipole and discrete cellular descriptions use different expressions for the induction of the dipole strength. In the classical discrete dipole description the dipole strengths, are induced according to

$$\mathbf{p}_i = \overleftrightarrow{\alpha}_i^{\text{cell}} \mathbf{E}_{\text{Loc},i}, \tag{4}$$

where $\overleftrightarrow{\alpha}_i^{\text{cell}}$ is the (local) polarizability tensor for cell i and $\mathbf{E}_{\text{Loc},i}$ the local electromagnetic field in this cell, defined by

$$\mathbf{E}_{\text{Loc},i} = \mathbf{E}_{\text{Ext}}(\mathbf{r}_i) + \sum_{j \neq i} \overleftrightarrow{\mathbf{t}}_{ij} \mathbf{p}_j, \tag{5}$$

where $\overleftrightarrow{\mathbf{t}}_{ij}$ represents the *transfer tensor* [10] for the dipole dipole interaction. Eq. (5) leaves out the intracellular transfer tensor $\overleftrightarrow{\mathbf{t}}_{ii}$, containing the electromagnetic self-interaction. The necessity of this omission is clear from the derivation of the Lorentz–Lorenz rule.

In contrast, the DCM makes use of nonlocal induction and does take the electromagnetic self-interaction into account. Therefore, the local field has to be replaced by the average field $\mathbf{E}_{\text{Av},i}$, which relates to the local field as

$$\mathbf{E}_{\text{Av},i} = \mathbf{E}_{\text{Loc},i} + \overleftrightarrow{\mathbf{t}}_{ii} \mathbf{p}_i, \tag{6}$$

where $\overleftrightarrow{\mathbf{t}}_{ii}$ is as defined and used in Ref. [18]. We recall from the introduction, that nonlocal induction means that the dipole strength of a cell will depend also on the average fields in neighboring cells. This nonlocality, combined with the condition of linear response, necessarily ends up in the use of nonlocal polarizabilities. The nonlocal equivalent of induction principle (4) now becomes

$$\mathbf{p}_i = \sum_j \overleftrightarrow{\alpha}_{ij}^{\text{qm}} \mathbf{E}_{\text{Av},j}. \tag{7}$$

The crucial difference is in the second index j. Summation over this index brings in the total quantum mechanical influence of the surroundings of cell i on the induction. The nonlocal polarizabilities α_{ij}^{qm} can only be obtained through elaborate quantum mechanical explicit calculations, hence the label qm. Details will be given in a forthcoming paper [15]. The influence of nonlocal polarizabilities for inhomogeneous properties is decisive [18].

In general, the equations governing both discrete dipole and discrete cellular calculations can be written as a matrix equation. The notation and derivation of these equations requires composite vectors and matrices as discussed in Ref. [11]. We define the composite polarizability matrix A and transfer tensor matrix T by

$$[A]_{ij} = \overleftrightarrow{\alpha}_{ij},$$

$$[T]_{ij} = \overleftrightarrow{\mathbf{t}}_{ij}, \tag{8}$$

where the square brackets refer to a 3×3 block part of the matrix. A visualization of the polarizability matrix A is shown in Fig. 1, indicating the difference between local and nonlocal induction. The polarizability matrix is, in general, full for the DCM. In all cases, both discrete cellular and discrete dipole, the solution can be obtained from the matrix equation

$$|\mathbf{P}| = [\mathbf{1} - AT]^{-1} A |\mathbf{E}_{\text{Ext}}|. \tag{9}$$

For the discrete dipole method the following matrix equation is preferred:

$$|\mathbf{P}| = [A^{-1} - T]^{-1} |\mathbf{E}_{\text{Ext}}|. \tag{10}$$

The advantage is that in this case the inverse of A is easily obtained. The disadvantage is that Eq. (10) cannot handle the vacuum case. Upon solution of the source terms $\mathbf{p}_i$ from Eq. (9), we have to obtain the measurable quantities such as

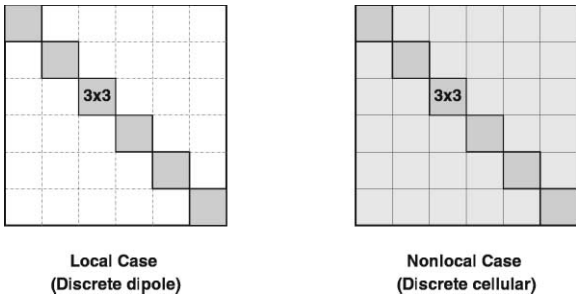

Fig. 1. Typical local and nonlocal polarizability matrices.

reflection coefficients from the remote field $\mathbf{E}_{\mathrm{Rem}}$, given by [11]

$$\mathbf{E}_{\mathrm{Rem}}(\mathbf{R}) = \frac{k^2 \mathrm{e}^{\mathrm{i}kR}}{4\pi\varepsilon_0 R}[\overleftrightarrow{\mathbf{1}} - \hat{\mathbf{R}}\hat{\mathbf{R}}^{\mathrm{T}}] \sum_{j=1}^{N} \mathrm{e}^{-\mathrm{i}k\hat{\mathbf{R}}\mathbf{r}_j}\mathbf{p}_j. \tag{11}$$

Eqs. (9)–(11) can handle the optical response of an arbitrary finite cluster of dipoles. Larger systems, such as semi-infinite ones, can only be treated if they obey some kind of translational symmetry and this at the expense of far more complex mathematics.

3. Translational symmetry and its influence

For bulk cubic symmetric systems under static conditions (Lorentz–Lorenz) nonlocal induction brings hardly anything new. Since all dipoles and average fields are the same then for every point i of the lattice, we have

$$\mathbf{p}_0 = \overleftrightarrow{\alpha}_{\mathrm{B}}^{\mathrm{qm}} \mathbf{E}_{\mathrm{Av},0},$$

$$\overleftrightarrow{\alpha}_{\mathrm{B}}^{\mathrm{qm}} = \sum_j \overleftrightarrow{\alpha}_{0j}^{\mathrm{qm}}, \tag{12}$$

where the index 0 is an arbitrary site of the lattice. Using Eq. (6) we can rewrite this result as

$$\mathbf{p}_0 = \overleftrightarrow{\alpha}_{\mathrm{B}}^{\mathrm{cell}} \mathbf{E}_{\mathrm{Loc},0},$$

$$\overleftrightarrow{\alpha}_{\mathrm{B}}^{\mathrm{cell}} = [(\overleftrightarrow{\alpha}_{\mathrm{B}}^{\mathrm{qm}})^{-1} - \overleftrightarrow{\mathbf{t}}_{ii}]^{-1}. \tag{13}$$

This new bulk polarizability $\overleftrightarrow{\alpha}_{\mathrm{B}}^{\mathrm{cell}}$ is indistinguishable from the polarizability used in the original Lorentz–Lorenz derivation. Hence the nonlocal equivalent of the Lorentz–Lorenz equation (isotropic case) remains the same

$$\left(\frac{\varepsilon - 1}{\varepsilon + 2}\right) = \frac{\alpha_{\mathrm{B}}^{\mathrm{cell}}}{3V_{\mathrm{WS}}\varepsilon_0}. \tag{14}$$

Here, ε is the relative bulk dielectric constant and V_{WS} the volume of the bulk Wigner–Seitz cell. As a result dispersionless homogeneous bulk properties will not reflect quantum mechanical nonlocal behavior. This kind of nonlocality can be manifested in the anisotropic properties of surfaces or in the spatial dispersion of the bulk.

Parallel translational symmetry is the only kind of symmetry left for surfaces and interfaces. If these systems obey such symmetry, it becomes feasible to treat their dynamic response. They are made from regular lattice planes defined by

$$\mathbf{s}_{rs} = r\mathbf{s}_1 + s\mathbf{s}_2, \tag{15}$$

where $\mathbf{s}_1$ and $\mathbf{s}_2$ are the two vectors spanning the plane. The pair (r, s) will be contracted into a single generalized index l. The system will be exposed to an external plane wave

$$\mathbf{E}(\mathbf{r}) = \mathbf{E}_0 \mathrm{e}^{\mathrm{i}\mathbf{k}\mathbf{r}}. \tag{16}$$

Following the electromagnetic wave in the plane will yield the same situation for all sites, if the time interval $\Delta t = t - t'$ needed for the wave to go from the origin to a site l, is properly accounted for. Any response $\mathbf{U}$ of a lattice site has to obey then

$$\mathbf{U}(\mathbf{s}_l, t) = \mathbf{U}(\mathbf{0}, t') = \mathbf{U}(\mathbf{0})\mathrm{e}^{\mathrm{i}\omega\Delta t} \tag{17}$$

for a driving frequency ω and time difference Δt, given by

$$\Delta t = \frac{\hat{\mathbf{k}}\mathbf{s}_l}{c} = \frac{\mathbf{k}_{\parallel}\mathbf{s}_l}{\omega}, \tag{18}$$

where $\mathbf{k} = (\mathbf{k}_{\parallel}, k_{\perp})$, $\omega = ck$ and the orientations $\parallel$ and $\perp$ are parallel and perpendicular to the plane, respectively. This yields the final expression

$$\mathbf{U}(\mathbf{s}_l) = \mathbf{U}(\mathbf{0})\mathrm{e}^{\mathrm{i}\mathbf{k}_{\parallel}\mathbf{s}_l}. \tag{19}$$

Different from the discrete cellular case, we have to apply this symmetry now to both the dipole strength $\mathbf{p}_l$ and the average field $\mathbf{E}_{\mathrm{Av},l}$.

3.1. Slabs

Translational symmetry enables us to treat directly slabs composed of crystalline lattice planes. As in Ref. [11] we select in each plane a **0**-site and call it the *characteristic site* with characteristic index I. Due to parallel translational symmetry, only quantities belonging to characteristic sites I play a role. The situation is shown in Fig. 2. We have applied in Ref. [11] parallel translational symmetry first to the dipole strengths

$$\mathbf{p}_l = \mathbf{p}_0 \mathrm{e}^{\mathrm{i}\mathbf{k}_{\parallel}\mathbf{s}_l}. \tag{20}$$

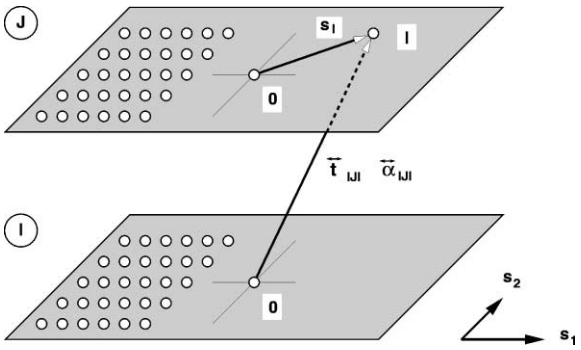

Fig. 2. Geometrical aspects of the nonlocal interactions between two planes of dipoles.

From this we obtain the following expression for the average field:

$$\mathbf{E}_{\mathrm{Av},I} = \mathbf{E}_{\mathrm{Ext}}(\mathbf{r}_I) + \sum_{J\neq I} \overleftrightarrow{\mathbf{f}}_{IJ}\mathbf{p}_J + \overleftrightarrow{\mathbf{f}}_{II}\mathbf{p}_I. \tag{21}$$

The tensor quantities $\overleftrightarrow{\mathbf{f}}_{IJ}$ are called interplanar transfer tensors if $I \neq J$ and intraplanar if $I = J$. Efficient expressions for these transfer tensors have been developed by Litzman [5–9], by us [10,11] and several other authors. When these expressions are to be used for the nonlocal case, the electromagnetic self-interaction $\mathbf{t}_{ii}$ needs to be added separately to the intraplanar transfer tensor. The transfer tensors are key components in any discrete treatment of crystalline lattice systems. What is new for the discrete cellular approach is that parallel translational symmetry is also applied to the average field

$$\mathbf{E}_{\mathrm{Av}}(\mathbf{s}_l) = \mathbf{E}_{\mathrm{Av}}(\mathbf{0})\mathrm{e}^{\mathrm{i}\mathbf{k}_\parallel \mathbf{s}_l}. \tag{22}$$

We use now this result in Eq. (7) to obtain

$$\mathbf{p}_I = \sum_J \overleftrightarrow{\alpha}^{\mathrm{Pl}}_{IJ}(\mathbf{k})\mathbf{E}_{\mathrm{Av},J},$$

$$\overleftrightarrow{\alpha}^{\mathrm{Pl}}_{IJ}(\mathbf{k}) = \sum_l \overleftrightarrow{\alpha}_{IJl}\mathrm{e}^{\mathrm{i}\mathbf{k}_\parallel \mathbf{s}_l}, \tag{23}$$

where $\mathbf{E}_{\mathrm{Av},J}$ is the average field at the characteristic site J and $\overleftrightarrow{\alpha}^{\mathrm{Pl}}$ is the *planar polarizability*. The most remarkable result of nonlocality is the $\mathbf{k}$-dependence of the planar polarizability in Eq. (23). Due to parallel translational symmetry only characteristic sites need to be considered and a minor index suffices. Exactly, as for a cluster of dipoles we define a polarizability matrix A and transfer tensor matrix F

$$[A(\mathbf{k})]_{ij} = \overleftrightarrow{\alpha}^{\mathrm{Pl}}_{ij}(\mathbf{k}),$$

$$[F]_{ij} = \overleftrightarrow{\mathbf{f}}_{ij}. \tag{24}$$

Now matrix A consists of planar polarizabilities and matrix F consists of planar transfer tensors $\mathbf{f}$. They replace the dipole transfer tensors $\mathbf{t}$ of the cluster case. Eq. (24) describes an arbitrary planar slab system for the two types of discrete modeling. As before we obtain the source terms $\mathbf{p}_i$ from the matrix equation

$$|\mathbf{P}| = [\mathbf{1} - A(\mathbf{k})F]^{-1}A(\mathbf{k})|\mathbf{E}_{\mathrm{Ext}}|. \tag{25}$$

This equation is suited for slabs, but semi-infinite systems have to be dealt with differently.

4. Semi-infinite systems

The double cell technique introduced in Ref. [11], can be extended to nonlocal semi-infinite systems, provided there is a finite range of nonlocality. This range implies that the (quantum mechanical) nonlocality extends over Y bulk unit cells. The geometric aspects of the double cell technique are shown in Fig. 3. The technique exploits the remnant periodicity in the perpendicular direction deep below the surface. There characteristic dipole sites $\mathbf{r}_{vV}$ obey bulk geometry according to

$$\mathbf{r}_{vV} = \mathbf{r}^{\mathrm{B}}_v + \mathbf{d}_{\mathrm{S}} + V\mathbf{s}_3. \tag{26}$$

This holds for all dipole sites outside the free surface layer. $V = 0$ gives the first bulk cell, with origin at $\mathbf{d}_{\mathrm{S}} = \mathbf{d}^{\mathrm{f}}_{\mathrm{S}} + N^{\mathrm{B}}_{\mathrm{S}}\mathbf{s}_3$. The N_{B} dipoles of the bulk unit cell have sites $\mathbf{r}^{\mathrm{B}}_v$, index v running from 1 to N_{B}. The semi-infinite system consists entirely of planes obeying the parallel translational symmetry described before. The bulk unit cell uses the vector $\mathbf{s}_3$ in addition to the vectors $\mathbf{s}_1, \mathbf{s}_2$. For the double cell technique, we need to consider two kinds of dipoles: bulk and surface ones.

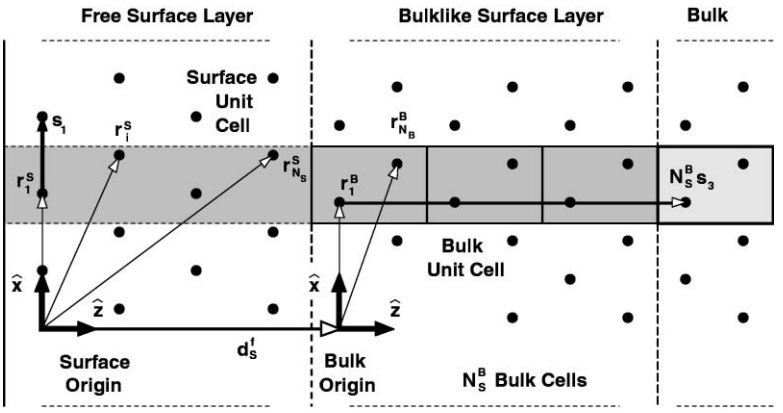

Fig. 3. Double cell geometry. The surface layer comprises a free and bulklike part. The bulklike part matches the free surface layer to the normal mode regime (bulk).

4.1. Bulk dipoles

We start with the vVth *bulk dipole*, given by

$$\mathbf{p}_{vV} = \sum_{X=V-Y}^{V+Y} \sum_{x=1}^{N_B} \overleftrightarrow{\alpha}^{B,Pl}_{vVxX}(\mathbf{k}) \mathbf{E}^{xX}_{Av}. \tag{27}$$

The polarizabilities $\overleftrightarrow{\alpha}^{B,Pl}_{vVxX}(\mathbf{k})$ each obey Eq. (23), where V has to exceed the value of the nonlocal bulk range Y. Since V is arbitrary, this imposes no limitation. The bulk average field is given by

$$\begin{aligned}\mathbf{E}^{xX}_{Av} = {} & E_0 \hat{\mathbf{e}} e^{i\mathbf{k}\mathbf{r}_{xX}} + \sum_{j=1}^{N_S} \overleftrightarrow{\mathbf{f}}_{xXj} \mathbf{p}_j \\ & + \sum_{w=1}^{N_B} \left[\sum_{W=0}^{X-1} \overleftrightarrow{\mathbf{f}}_{xXwW} \mathbf{p}_{wW} + \overleftrightarrow{\mathbf{f}}_{xXw} \mathbf{p}_{wX} \right. \\ & \left. + \sum_{W=X+1}^{\infty} \overleftrightarrow{\mathbf{f}}_{xXwW} \mathbf{p}_{wW} \right], \end{aligned} \tag{28}$$

where we have written vw instead of $vVwV$. The surface unit cell (has slightly darker shading in Fig. 3) contains N_S dipoles. It is split into a free surface layer and a bulk-like surface layer [11]. Dipoles in the bulk-like surface layer are at bulk geometry positions, as given by Eq. (26). This layer accounts for the matching of bulk and surface. The remnant bulk perpendicular periodicity enables, as in Ref. [11], the use of normal modes

$$\mathbf{p}_{vV} = \sum_{m=1}^{M} v_m \mathbf{u}_{mv} e^{iV\mathbf{k}_m \mathbf{s}_3}. \tag{29}$$

The number of normal modes is given by M. The dimensionless v_m is the normal mode strength, $\mathbf{u}_{mv}$ the normal mode vector and $\mathbf{k}_m$ the normal mode wave vector. As in Ref. [11], we use Ewald's threefold integral transform to expand the planar transfer tensors. As a result, the expression for the average field (28) decomposes into "channels", belonging to wave vectors $\mathbf{k}$, $\mathbf{k}_{pq}$ and $\mathbf{k}_m$. After some lengthy, but straightforward derivation we obtain

$$\begin{aligned}\mathbf{E}^{xX}_{Av} = {} & \mathbf{E}^{x}_{Ext}(\mathbf{k}) e^{iX\mathbf{k}\mathbf{s}_3} + \sum_{pq}^{\infty} \mathbf{E}^{x}_{>}(\mathbf{k}_{pq}) e^{iX\mathbf{k}_{pq}\mathbf{s}_3} \\ & + \sum_{m=1}^{M} \mathbf{E}^{x}_{B}(\mathbf{k}_m) e^{iX\mathbf{k}_m\mathbf{s}_3}. \end{aligned} \tag{30}$$

Each of the channel fields $\mathbf{E}^{x}_{Ext}(\mathbf{k})$, $\mathbf{E}^{x}_{>}(\mathbf{k}_{pq})$ and $\mathbf{E}^{x}_{B}(\mathbf{k}_m)$ is controlled by a different exponential of X and they are defined as (underline refers to reflection)

$$\mathbf{E}^{x}_{Ext}(\mathbf{k}) = E_0 \hat{\mathbf{e}} e^{i\mathbf{k}(\mathbf{r}^B_x + \mathbf{d}_S)},$$

$$\begin{aligned}\mathbf{E}^{x}_{>}(\mathbf{k}_{pq}) = {} & \left[\sum_{j=1}^{N_S} e^{i\mathbf{k}_{pq}(\mathbf{r}^B_x + \mathbf{d}_S - \mathbf{r}_j)} \overleftrightarrow{\mathbf{d}}_{pq} \mathbf{p}_j \right. \\ & \left. + \sum_{w=1}^{N_B} \sum_{m=1}^{M} v_m \overleftrightarrow{\mathbf{d}}_{pq} \mathbf{u}_{mw} \left[\frac{e^{i\mathbf{k}_{pq}(\mathbf{r}^B_x - \mathbf{r}^B_w)}}{1 - e^{i(\mathbf{k}_m - \mathbf{k}_{pq})\mathbf{s}_3}} \right] \right], \end{aligned}$$

$$\mathbf{E}_{\mathrm{B}}^{x}(\mathbf{k}_m) = v_m \sum_{w=1}^{N_{\mathrm{B}}} \left[\overleftrightarrow{\mathbf{f}}_{xw} + \sum_{pq}^{\infty} \left[\frac{\mathrm{e}^{\mathrm{i}\mathbf{k}_{pq}(\mathbf{r}_x^{\mathrm{B}} - \mathbf{r}_w^{\mathrm{B}})}}{\mathrm{e}^{\mathrm{i}(\mathbf{k}_m - \mathbf{k}_{pq})\mathbf{s}_3} - 1} \overleftrightarrow{\mathbf{d}}_{pq} + \frac{\mathrm{e}^{\mathrm{i}\underline{\mathbf{k}}_{pq}(\mathbf{r}_x^{\mathrm{B}} - \mathbf{r}_w^{\mathrm{B}})}}{\mathrm{e}^{\mathrm{i}(\underline{\mathbf{k}}_{pq} - \mathbf{k}_m)\mathbf{s}_3} - 1} \overleftrightarrow{\underline{\mathbf{d}}}_{pq} \right] \right] \mathbf{u}_{mw}. \tag{31}$$

For the *transverse projectors* $\overleftrightarrow{\mathbf{f}}_{pq}$ of Ref. [11] we have to use here the expression

$$\overleftrightarrow{\mathbf{d}}_{pq} = \frac{\mathrm{i}}{2\varepsilon_0 |\mathbf{s}_1 \times \mathbf{s}_2|} \frac{k^2 \overleftrightarrow{\mathbf{1}} - \mathbf{k}_{pq}\mathbf{k}_{pq}^{\mathrm{T}}}{\kappa_{pq}}. \tag{32}$$

The channel fields greatly facilitate evaluation of the average fields. Replacing the index X by $V + X$, we obtain from the induction equation (27)

$$\begin{aligned} &\sum_{m=1}^{M} v_m \mathbf{u}_{mv} \mathrm{e}^{\mathrm{i}V\mathbf{k}_m\mathbf{s}_3} \\ &= \sum_{X=-Y}^{+Y} \sum_{x=1}^{N_{\mathrm{B}}} \overleftrightarrow{\alpha}_{vVx(V+X)}^{\mathrm{B,Pl}}(\mathbf{k}) \mathbf{E}_{\mathrm{Av}}^{x(V+X)} \\ &= \sum_{x=1}^{N_{\mathrm{B}}} \left[\overleftrightarrow{\alpha}_{vx}^{Y}(\mathbf{k}) \mathbf{E}_{\mathrm{Ext}}^{x}(\mathbf{k}) \mathrm{e}^{\mathrm{i}V\mathbf{k}\mathbf{s}_3} \right. \\ &\quad + \sum_{pq}^{\infty} \overleftrightarrow{\alpha}_{vx}^{Y}(\mathbf{k}_{pq}) \mathbf{E}_{>}^{x}(\mathbf{k}_{pq}) \mathrm{e}^{\mathrm{i}V\mathbf{k}_{pq}\mathbf{s}_3} \\ &\quad \left. + \sum_{m=1}^{M} \overleftrightarrow{\alpha}_{vx}^{Y}(\mathbf{k}_m) \mathbf{E}_{\mathrm{B}}^{x}(\mathbf{k}_m) \mathrm{e}^{\mathrm{i}V\mathbf{k}_m\mathbf{s}_3} \right], \end{aligned} \tag{33}$$

where we have defined, using bulk symmetry, the *nonlocal bulk polarizabilities* $\overleftrightarrow{\alpha}_{vx}^{Y}(\mathbf{k})$ as

$$\overleftrightarrow{\alpha}_{vx}^{Y}(\mathbf{k}) = \sum_{X=-Y}^{+Y} \overleftrightarrow{\alpha}_{vxX}^{\mathrm{B,Pl}}(\mathbf{k}) \mathrm{e}^{\mathrm{i}X\mathbf{k}\mathbf{s}_3}. \tag{34}$$

This use of infinitely many $\mathbf{k}$-dependent bulk polarizability matrices in the nonlocal case is the main distinction as compared to the local case where only one bulk polarizability matrix is used. If we filter out from Eq. (33) the independent channels, most of these matrices will vanish. The $\mathbf{k}_m$-channel enables us to determine the key normal mode parameters $\mathbf{u}_{mv}$ and $\mathbf{k}_m$

$$\mathbf{u}_{mv} = \sum_{x=1}^{N_{\mathrm{B}}} \overleftrightarrow{\alpha}_{vx}(\mathbf{k}_m) \sum_{w=1}^{N_{\mathrm{B}}} \left[\overleftrightarrow{\mathbf{f}}_{xw} + \sum_{pq}^{\infty} \left[\frac{\mathrm{e}^{\mathrm{i}\mathbf{k}_{pq}(\mathbf{r}_x^{\mathrm{B}} - \mathbf{r}_w^{\mathrm{B}})}}{\mathrm{e}^{\mathrm{i}(\mathbf{k}_m - \mathbf{k}_{pq})\mathbf{s}_3} - 1} \overleftrightarrow{\mathbf{d}}_{pq} + \frac{\mathrm{e}^{\mathrm{i}\mathbf{k}_{pq}(\mathbf{r}_x^{\mathrm{B}} - \mathbf{r}_w^{\mathrm{B}})}}{\mathrm{e}^{\mathrm{i}(\underline{\mathbf{k}}_{pq} - \mathbf{k}_m)\mathbf{s}_3} - 1} \overleftrightarrow{\underline{\mathbf{d}}}_{pq} \right] \right] \mathbf{u}_{mw}, \tag{35}$$

N_{B} independent vector equations will be obtained by varying the index v. This enables the introduction of the auxiliary $N_{\mathrm{B}} \times N_{\mathrm{B}}$ composite matrices A and F:

$$[A(\mathbf{k})]_{vx} = \overleftrightarrow{\alpha}_{vx}^{Y}(\mathbf{k}),$$

$$[F(\mathbf{k})]_{xw} = \overleftrightarrow{\mathbf{f}}_{xw} + \sum_{pq}^{\infty} \left[\frac{\mathrm{e}^{\mathrm{i}\mathbf{k}_{pq}(\mathbf{r}_x^{\mathrm{B}} - \mathbf{r}_w^{\mathrm{B}})}}{\mathrm{e}^{\mathrm{i}(\mathbf{k} - \mathbf{k}_{pq})\mathbf{s}_3} - 1} \overleftrightarrow{\mathbf{d}}_{pq} + \frac{\mathrm{e}^{\mathrm{i}\underline{\mathbf{k}}_{pq}(\mathbf{r}_x^{\mathrm{B}} - \mathbf{r}_w^{\mathrm{B}})}}{\mathrm{e}^{\mathrm{i}(\underline{\mathbf{k}}_{pq} - \mathbf{k})\mathbf{s}_3} - 1} \overleftrightarrow{\underline{\mathbf{d}}}_{pq} \right]. \tag{36}$$

Using these matrices, we can write Eq. (35) concisely as

$$M(\mathbf{k}_m)|\mathbf{u}| = [\mathbf{1} - A(\mathbf{k}_m)F(\mathbf{k}_m)]|\mathbf{u}| = |\mathbf{0}|, \tag{37}$$

where the matrix $M(\mathbf{k}_m)$ represents the bulk secular matrix. To search for the zeros $\mathbf{k}_m$ of the corresponding secular determinant and to obtain the normal mode vectors $\mathbf{u}_{mw}$, we use the procedure described already in Ref. [11]. For the normal mode strength v_m, it is enough to use the $\mathbf{k}_{00}$-channel (this channel happens to coincide with the $\mathbf{k}$-channel). From this forward propagating channel we obtain

$$\sum_{x=1}^{N_{\mathrm{B}}} \overleftrightarrow{\alpha}_{vx}^{Y}(\mathbf{k}) [\mathbf{E}_{\mathrm{Ext}}^{x}(\mathbf{k}) + \mathbf{E}_{>}^{x}(\mathbf{k})] = 0. \tag{38}$$

This equation can be recognized again as a matrix equation, being

$$A(\mathbf{k})[|\mathbf{E}_{\mathrm{Ext}}(\mathbf{k})| + |\mathbf{E}_{>}(\mathbf{k})|] = |\mathbf{0}|. \tag{39}$$

Since this matrix $A(\mathbf{k})$ is in general not singular, we can conclude immediately that

$$|\mathbf{E}_{\mathrm{Ext}}(\mathbf{k})| + |\mathbf{E}_{>}(\mathbf{k})| = |\mathbf{0}| \tag{40}$$

which is nothing else but the classical Ewald–Oseen extinction theorem. When the common

phase factor $\exp(\mathrm{i}\mathbf{k}\mathbf{r}_v^{\mathrm{B}})$ in the vth vector component of this composite equation is divided out [11], only a single vector equation is left finally

$$-\overleftrightarrow{\mathbf{d}}_{00}\left[\sum_{w=1}^{N_{\mathrm{B}}}\sum_{m=1}^{M} v_m\mathbf{u}_{mw}\left[\frac{\mathrm{e}^{-\mathrm{i}\mathbf{k}\mathbf{r}_w^{\mathrm{B}}}}{1-\mathrm{e}^{\mathrm{i}(\mathbf{k}_m-\mathbf{k})\mathbf{s}_3}}\right]+\sum_{j=1}^{N_{\mathrm{S}}}\mathrm{e}^{\mathrm{i}\mathbf{k}(\mathbf{d}_{\mathrm{S}}-\mathbf{r}_j)}\mathbf{p}_j\right]=E_0\hat{\mathbf{e}}\mathrm{e}^{\mathrm{i}\mathbf{k}\mathbf{d}_{\mathrm{S}}}. \tag{41}$$

Now we can proceed exactly as in Ref. [11] and obtain for the *forward bulk part of the double cell equations*

$$\frac{\mathrm{i}k^2}{2\varepsilon_0|\mathbf{s}_1\times\mathbf{s}_2|\,|k_z|}\left[-\sum_{m=1}^{M}(\hat{\mathbf{t}}^{\mathrm{T}}\mathbf{P}_m^{\mathrm{B}}(\mathbf{k}))v_m-\sum_{j=1}^{N_{\mathrm{S}}}\mathrm{e}^{\mathrm{i}\mathbf{k}(\mathbf{d}_{\mathrm{S}}-\mathbf{r}_j)}\hat{\mathbf{t}}^{\mathrm{T}}\mathbf{p}_j\right]=E_0\mathrm{e}^{\mathrm{i}\mathbf{k}\mathbf{d}_{\mathrm{S}}}(\hat{\mathbf{t}}^{\mathrm{T}}\hat{\mathbf{e}}),$$

$$\mathbf{P}_m^{\mathrm{B}}(\mathbf{k})=\frac{\sum_{w=1}^{N_{\mathrm{B}}}\mathrm{e}^{-\mathrm{i}\mathbf{k}\mathbf{r}_w^{\mathrm{B}}}\mathbf{u}_{mw}}{1-\exp(\mathrm{i}[\mathbf{k}_m-\mathbf{k}]\mathbf{d}_{\mathrm{B}})}, \tag{42}$$

where $\mathbf{P}_m^{\mathrm{B}}(\mathbf{k})$ is the *cumulative normal mode dipole strength*. That this result is identical for local and nonlocal cases, is obvious since nonlocality affects only the polarizability matrix, which drops out already from the equations at a very early stage.

4.2. Surface dipoles

Typical for the nonlocal case is the *nonlocal extension layer*, consisting of the first Y bulk unit cells of the normal mode region, as depicted in Fig. 4. These cells exert a *direct influence on the dipoles of the surface layer*. We consider an arbitrary dipole $\mathbf{p}_i$ located in the surface layer and apply the nonlocal induction rule (23)

$$\mathbf{p}_i=\sum_{l=1}^{N_{\mathrm{S}}}\overleftrightarrow{\alpha}_{il}(\mathbf{k})\mathbf{E}_{\mathrm{Av}}^{l}+\sum_{X=0}^{Y}\sum_{x=1}^{N_{\mathrm{B}}}\overleftrightarrow{\alpha}_{ixX}(\mathbf{k})\mathbf{E}_{\mathrm{Av}}^{xX}. \tag{43}$$

In the usual way Eq. (43) turns into a matrix equation

$$|\mathbf{P}|=A(\mathbf{k})|\mathbf{E}_{\mathrm{Av}}|. \tag{44}$$

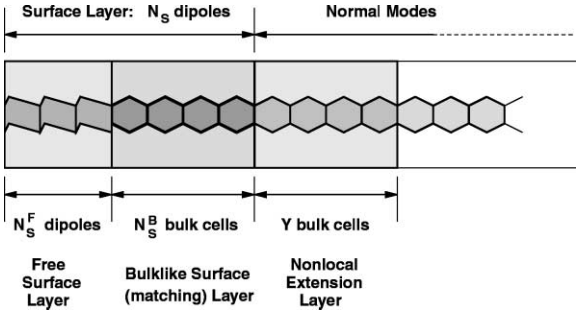

Fig. 4. Nonlocal surface geometry. The nonlocal extension layer belongs to the normal mode regime (bulk), but affects the surface directly.

Special attention needs to be paid to the dimensions. The dipole vector contains N_{S} vectors, the matrix $N_{\mathrm{S}}\times(N_{\mathrm{S}}+Y*N_{\mathrm{B}})$ subtensors and the average field vector $N_{\mathrm{S}}+Y*N_{\mathrm{B}}$ vectors. The expression for the average field in the surface layer and in the nonlocal extension layer is different. The surface average fields can be taken from Ref. [11]

$$\mathbf{E}_{\mathrm{Av}}^{l}=E_0\hat{\mathbf{e}}\mathrm{e}^{\mathrm{i}\mathbf{k}\mathbf{r}_l}+\sum_{j=1}^{N_{\mathrm{S}}}\overleftrightarrow{\mathbf{f}}_{lj}\mathbf{p}_j+\sum_{m=1}^{M}\underline{\mathbf{h}}_{lm}v_m,$$

$$\underline{\mathbf{h}}_{lm}=\sum_{w=1}^{N_{\mathrm{B}}}\sum_{pq}^{\infty}\left[\frac{\mathrm{e}^{\mathrm{i}\underline{\mathbf{k}}_{pq}(\mathbf{r}_l-\mathbf{r}_w^{\mathrm{B}}-\mathbf{d}_{\mathrm{S}})}}{1-\mathrm{e}^{\mathrm{i}(\mathbf{k}_m-\underline{\mathbf{k}}_{pq})\mathbf{s}_3}}\right]\overleftrightarrow{\underline{\mathbf{d}}}_{pq}\mathbf{u}_{mw}. \tag{45}$$

For the average fields in the nonlocal extension layer we can use Eqs. (30) and (31) in a different notation

$$\mathbf{E}_{\mathrm{Av}}^{xX}=E_0\hat{\mathbf{e}}\mathrm{e}^{\mathrm{i}\mathbf{k}[\mathbf{r}_x^{\mathrm{B}}+\mathbf{d}_{\mathrm{S}}+X\mathbf{s}_3]}+\sum_{j=1}^{N_{\mathrm{S}}}\overleftrightarrow{\mathbf{f}}_{xXj}\mathbf{p}_j+\sum_{m=1}^{M}\mathbf{h}_{xXm}v_m,$$

$$\mathbf{h}_{xXm}=\mathrm{e}^{\mathrm{i}X\mathbf{k}_m\mathbf{s}_3}\sum_{w=1}^{N_{\mathrm{B}}}\left[\overleftrightarrow{\mathbf{f}}_{xw}+\sum_{pq}^{\infty}\left[\left[\frac{\mathrm{e}^{\mathrm{i}\mathbf{k}_{pq}(\mathbf{r}_x^{\mathrm{B}}-\mathbf{r}_w^{\mathrm{B}})}(\mathrm{e}^{\mathrm{i}X(\mathbf{k}_{pq}-\mathbf{k}_m)\mathbf{s}_3}-1)}{1-\mathrm{e}^{\mathrm{i}(\mathbf{k}_m-\mathbf{k}_{pq})\mathbf{s}_3}}\right]\overleftrightarrow{\mathbf{d}}_{pq}+\left[\frac{\mathrm{e}^{\mathrm{i}\underline{\mathbf{k}}_{pq}(\mathbf{r}_x^{\mathrm{B}}-\mathbf{r}_w^{\mathrm{B}})}}{\mathrm{e}^{\mathrm{i}(\underline{\mathbf{k}}_{pq}-\mathbf{k}_m)\mathbf{s}_3}-1}\right]\overleftrightarrow{\underline{\mathbf{d}}}_{pq}\right]\right]\mathbf{u}_{mw}. \tag{46}$$

Combination of Eqs. (45) and (46) yields the matrix equation

$$|\mathbf{E}_{\mathrm{Av}}|=|\mathbf{E}_{\mathrm{Ext}}|+F|\mathbf{P}|+h|v|, \tag{47}$$

where the matrix F is as defined in Eq. (24). The size of composite vectors $\mathbf{E}_{\mathrm{Av}}$ and $\mathbf{E}_{\mathrm{Ext}}$ is $N_{\mathrm{S}} + Y * N_{\mathrm{B}}$ vectors. Composite vector $\mathbf{P}$ contains N_{S} vectors, whereas composite vector v contains only M complex numbers. The dimensions of the matrices are in agreement with those of the vectors. Combination of Eqs. (44) and (47) gives the surface part of the nonlocal double cell interaction equations

$$[\mathbf{1} - A(\mathbf{k})F]|\mathbf{P}| - A(\mathbf{k})h|v| = A(\mathbf{k})|\mathbf{E}_{\mathrm{Ext}}|. \tag{48}$$

The $N_{\mathrm{S}} \times N_{\mathrm{S}}$ composite matrix $\mathbf{1} - AF$ is the SS-part of the nonlocal double cell interaction matrix. It is by far the largest part of this matrix. Finally, Eqs. (42) and (48) have to be combined to give the full nonlocal interaction matrix M

$$\begin{vmatrix} M_{\mathrm{SS}} & M_{\mathrm{SB}} \\ M_{\mathrm{BS}} & M_{\mathrm{BB}} \end{vmatrix} \begin{vmatrix} \mathbf{p}_i \\ v_m \end{vmatrix} = \begin{vmatrix} A\mathbf{E}_{\mathrm{Ext},i} \\ \mathbf{t}_n^{\mathrm{T}}\mathbf{E}_{\mathrm{Ext}}^{\mathrm{B}} \end{vmatrix}. \tag{49}$$

The explicit expressions for the components of the matrix are given by

$$M_{\mathrm{SS}} = \mathbf{1} - A(\mathbf{k})F, \qquad M_{\mathrm{SB}} = -A(\mathbf{k})h,$$
$$M_{\mathrm{BS},nj} = \frac{\mathrm{i}k^2\hat{\mathbf{t}}_n^{\mathrm{T}}}{2\varepsilon_0|\mathbf{s}_1 \times \mathbf{s}_2|\,|k_z|}, \qquad M_{\mathrm{BB},nm} = \frac{\mathrm{i}k^2\hat{\mathbf{t}}_n^{\mathrm{T}}\mathbf{P}_m^{\mathrm{B}}(\mathbf{k})}{2\varepsilon_0|\mathbf{s}_1 \times \mathbf{s}_2|\,|k_z|}, \tag{50}$$

Although quantum induction heavily perturbs the derivation, the final result is surprisingly very manageable and hardly more complicated than the local equivalent. Obviously, the local case is a subcase of the nonlocal one.

4.3. Extra normal modes

In our previous local publications [10,11] only two normal modes, always in the close vicinity of the Fresnel solutions, had to be used for the bulk region. Unexpectedly, in doing calculations on GaAs [18] it turned out that sometimes more modes were required. We will treat here how these *extra normal modes*, also derived from Eq. (37), have to be incorporated into the description. The extra normal modes have to be derived from pq channels, different from the 00 channel. Using the full bulk Eq. (33), we arrive for one such pq channel at

$$A(\mathbf{k}_{pq})\ \mathbf{E}_{>}^{x}(\mathbf{k}_{pq}) = 0. \tag{51}$$

Since the matrices $A(\mathbf{k}_{pq})$ will be in general nonsingular, we have again

$$\mathbf{E}_{>}^{k}(\mathbf{k}_{pq}) = 0. \tag{52}$$

After elimination of a common phase factor $\exp(\mathrm{i}\mathbf{k}_{pq}\mathbf{r}_v^{\mathrm{B}})$, the expression for $\mathbf{E}_{>}^{k}(\mathbf{k}_{pq})$ Eq. (31) yields

$$\overleftrightarrow{\mathbf{d}}_{pq}\left[\sum_{j=1}^{N_{\mathrm{S}}^1} \mathrm{e}^{\mathrm{i}\mathbf{k}_{pq}(\mathbf{d}_{\mathrm{S}}-\mathbf{r}_j)}\mathbf{p}_j + \sum_{w=1}^{N_{\mathrm{B}}}\sum_{m=1}^{M} v_m\mathbf{P}_m^{\mathrm{B}}(\mathbf{k}_{pq})\right] = 0. \tag{53}$$

Due to the projection character of the transverse projectors $\overleftrightarrow{\mathbf{d}}_{pq}$ [11] the three additional rows (53) of the double cell matrix will be dependent. We have to filter out the independent part, using a projection vector $\hat{\mathbf{t}}_{pq}$, obeying

$$\hat{\mathbf{t}}_{pq}^{\mathrm{T}}\mathbf{k}_{pq} = 0. \tag{54}$$

For any arbitrary vector $\mathbf{y}$, to which we apply $\mathbf{d}_{pq}$ and project the result onto such $\hat{\mathbf{t}}_{pq}$, we get (see Ref. [11])

$$\hat{\mathbf{t}}_{pq}^{\mathrm{T}}\ \overleftrightarrow{\mathbf{d}}_{pq}\mathbf{y} = \frac{\mathrm{i}}{2\varepsilon_0|\mathbf{s}_1 \times \mathbf{s}_2|\kappa_{pq}}[\hat{\mathbf{t}}_{pq}^{\mathrm{T}}\mathbf{y}]. \tag{55}$$

Using this result for the projection, Eq. (53) becomes

$$\sum_{j=1}^{N_{\mathrm{S}}^1} \mathrm{e}^{\mathrm{i}\mathbf{k}_{pq}(\mathbf{d}_{\mathrm{S}}-\mathbf{r}_j)}\hat{\mathbf{t}}_{pq}^{\mathrm{T}}\mathbf{p}_j + \sum_{w=1}^{N_{\mathrm{B}}}\sum_{m=1}^{M} v_m\hat{\mathbf{t}}_{pq}^{\mathrm{T}}\mathbf{P}_m^{\mathrm{B}}(\mathbf{k}_{pq}) = 0. \tag{56}$$

Now we are left with a single row to be added to the double cell matrix. Addition of more columns in the surface part follows the derivation of Eq. (46). We have used two of these extra normal modes, obtained from the 10 and 02 channel and requiring the z-component of the corresponding $\hat{\mathbf{t}}_{pq}$ to be zero. Then condition (54) and normalization suffice to determine uniquely the $\hat{\mathbf{t}}_{pq}$'s. One has to be keen in selecting the additional rows, since there can be more pairs pq belonging to the same κ_{pq}. Such pairs can result easily into two dependent rows and cause a singular double cell interaction matrix.

4.4. Remote propagator

The (planar) remote propagator $\overleftrightarrow{\mathbf{f}}_R(\mathbf{R})$ links the microscopic response as given by $\mathbf{p}_i$ and v_m to the electric fields $\mathbf{E}_{\mathrm{Rem}}$ at a remote point $\mathbf{R}$. This propagator is exactly the same as for the local case [11] and is given for the case of reflection by

$$\mathbf{E}_{\mathrm{Rem}}(\mathbf{R}) = \overleftrightarrow{\mathbf{f}}_R(\mathbf{R})\mathbf{P}(\underline{\mathbf{k}}),$$

$$\overleftrightarrow{\mathbf{f}}_R(\mathbf{R}) = \frac{\mathrm{i}e^{\mathrm{i}\underline{\mathbf{k}}\mathbf{R}}}{2\varepsilon_0|\mathbf{s}_1 \times \mathbf{s}_2|\,|k_z|}[k^2\mathbf{1} - \underline{\mathbf{k}}\underline{\mathbf{k}}^{\mathrm{T}}],$$

$$\mathbf{P}(\mathbf{k}) = \sum_{j=1}^{N_S} e^{-\mathrm{i}\mathbf{k}\mathbf{r}_j}\mathbf{p}_j + e^{-\mathrm{i}\mathbf{k}\mathbf{d}_S}\sum_{m=1}^{M} v_m\mathbf{P}_m^{\mathrm{B}}(\mathbf{k}). \qquad (57)$$

When the summation over m is left out, this expression treats the remote response of slabs also. The remote fields can be used to generate all kinds of expressions used to describe the experimental observations. Only as an example we give the expression for the reflection coefficient r_t, where t represents the direction of the analyzer:

$$r_t = \frac{\mathrm{i}k^2}{2\varepsilon_0|\mathbf{s}_1 \times \mathbf{s}_2|\,|k_z|}\left[\frac{\hat{\underline{\mathbf{t}}}^{\mathrm{T}}\mathbf{P}(\underline{\mathbf{k}})}{E_0}\right] \qquad (58)$$

the commonly used polarization directions s or p are just special cases of t.

5. Results

We have reported already DCM results for the reflectance anisotropy (RA) of the GaAs (1 1 0) surface elsewhere [18]. Here, we will compare these results with other published results and give some additional normal mode material.

We have used normal modes before [10,11,19], but did not discuss details. Since the extra normal modes in the case of GaAs are new, we have included Fig. 5 showing normal mode behavior. The wave vector $\mathbf{k}_m = (\mathbf{k}_\parallel, q_m)$ is along the (0 0 1) direction. Fig. 5 shows the zero-contours of the real and imaginary part of the secular determinant $||M||$, governing the bulk dynamic behavior, as a function of q_m. Each crossing of real and imaginary contours marks a normal mode. The figure has inversion symmetry and is periodic along the real axis, with period $2\pi/s_{3z}$. The search

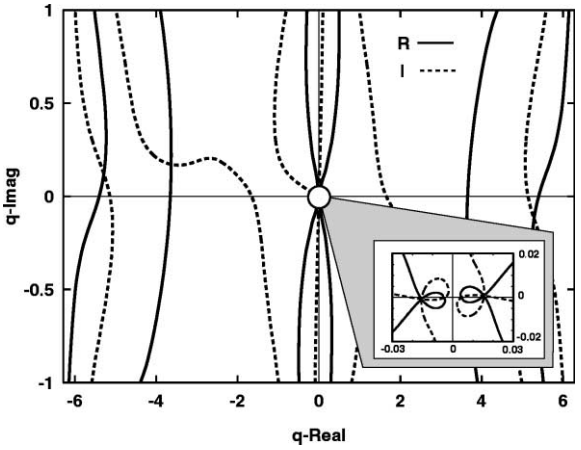

Fig. 5. Real and imaginary part zero-contours of $||M||$ for $\hbar\omega = 2.0$ eV. Inset: Fresnel solution region.

can be restricted for imaginary q_m-values to some suitably chosen cutoff value, because of damping.

The inset of Fig. 5 shows the common normal modes, always found in the close vicinity of the traditional Fresnel solutions. The intersections closest to the origin are singularities on the real axis and do not belong to normal modes. They occur, when in Eq. (36) the wave vector $\mathbf{k}_m$ coincides with $\mathbf{k}_{00} = \mathbf{k}$, the wave vector of the incoming beam. The two other crossings are Fresnel-type normal modes. These two solutions are very close to each other, but do not coincide, opposite to what Fresnel theory predicts. The discrepancy points to bulk spatial dispersion [20,21] and occurs for GaAs for all frequencies we have investigated. The two crossings left from the imaginary axis are extra normal modes.

For very low frequencies these extra normal modes are exactly at the boundary of the Brillouin zone, but can be ignored because of strong damping. From 1.1 eV two different extra normal modes, one being purely transverse ($\mathbf{u} \cdot \mathbf{k}_m = 0$), the other having a strong longitudinal component ($\mathbf{u} \cdot \mathbf{k}_m \neq 0$), start to move from the zone boundary towards the imaginary axis. At the start they are transparent, but above the bandgap at 1.5 eV they get increasingly absorbing. The extra modes preserve their transverse/longitudinal character for increasing energy. Their influence can be discarded above 2.6 eV, again because of damping.

The mode strength of the extra normal modes is smaller than those of the Fresnel-type modes, at 2.0 eV, for example, about 10%. This however, is enough to cause a visible modulation of the bulk microscopic response [18], when they are sufficiently transparent.

From Ref. [18] we have selected the RA data to compare them with experiment and results obtained with other well established methods. RA is the relative change in reflectance when the direction of polarization of perpendicularly incident light varies between the two symmetry axes of the surface. Very accurate measurements of RA have been obtained for the GaAs (1 1 0) surface by Esser et al. [22]. We show these experimental data and our DCM RA calculations in Fig. 6. We compare these results with the results of Pulci et al. [23], obtained by means of continuum theory. In the upper panel of Fig. 6 we show the continuum results obtained from an electronic structure calculation in the local density approximation (LDA), and in the lower panel results using the GW-approximation for the self-energy (LDA is a common approximation used in most of the present electronic structure calculations, where the exchange-correlation part of the effective one particle potential is a local functional of the density. Although this approximation is satisfying for the ground state, it fails to describe excited states correctly. The GW-approximation cures this problem by adding a next level of corrections to the LDA-treatment. These corrections embody the use of a screened self-energy, a Green function description and the first level of electron–hole pair treatment [24]). The DCM results are very close to experiment. The modulation of the continuum results is stronger than that observed experimentally. This holds particularly for the LDA results.

In [23] the main structures observed in the RA spectra of GaAs (1 1 0) have been given labels. In addition, we give the label "P" to the peak experimentally observed at 3.4 eV. The energetic positions of these structures for the experiment and the three types of calculation are given in Table 1. Our DCM calculations start from the ADF-BAND method of Baerends and te Velde [25,26], based on LDA. We have used a scissors operator of 0.399 eV in upward direction for the

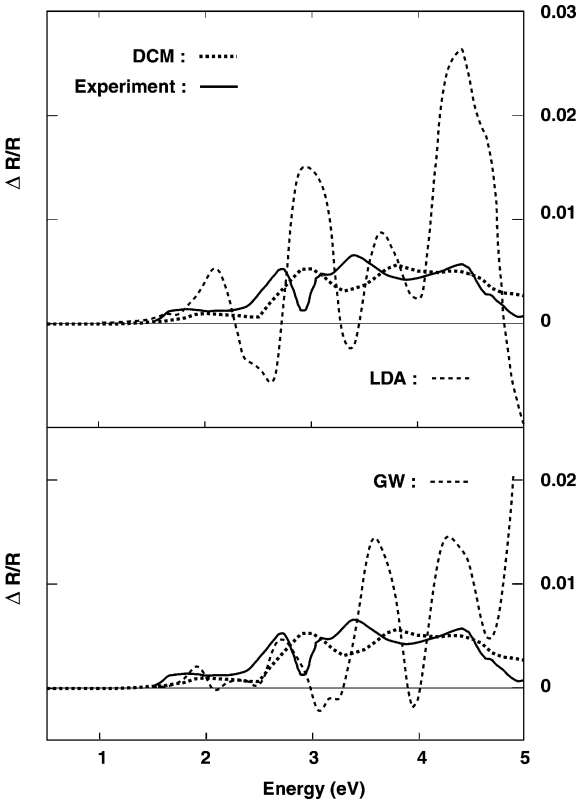

Fig. 6. Reflectance anisotropy: comparison between DCM and continuum results (LDA and GW, from Ref. [19]). For full explanation see text.

Table 1
Energy positions of main RA structures. LDA- and GW-type results from Ref. [23], Experimental data from Ref. [22]

	Expt	LDA	GW	DCM
S (max)	2.7 eV	1.8 eV	2.7 eV	2.9 eV
E_1 (min)	2.9 eV	2.3 eV	3.1 eV	3.3 eV
P (max)	3.4 eV	2.7 eV	3.6 eV	3.8 eV
E_0' (max)	4.4 eV	3.3 eV	4.3 eV	4.4 eV
E_2 (min)	4.9 eV	3.8 eV	4.8 eV	5.0 eV

bulk as compensation. The continuum LDA calculation has not been shifted. To obtain the proper energetic location of final state effects requires a method like GW (or Bethe–Salpeter or time dependent density functional theory (TD-DFT)). If we calculate the average shift in energy with respect to experiment for the structures listed in Table 1, we find an average shift of 0.88 eV for

LDA, a shift of 0.16 eV for GW and a shift of 0.22 eV for DCM. Obviously, the best agreement is obtained for GW. The large average shift for LDA had to be anticipated. The bulk scissors operator for DCM has been certainly effective.

The first motive behind DCM, however, is not a proper determination of the energetic location of spectral features, but of the absolute and relative intensities of those. It is clear from Fig. 6 that DCM outperforms easily the two continuum approaches LDA and GW in this respect. The signal modulation for the two continuum calculations is far above the experimentally observed one. Especially, the shape of the spectra is much better replicated by DCM. It is unlikely that the differences between the continuum calculations and DCM have to be ascribed to differences in the wave functions, so the difference has to be methodological. In that sense the methods are too far apart to allow for a direct comparison. Only for DCM we can mention that "switching off" quantum induction results in far worse agreement between theory and experiment [18]. So within DCM quantum induction, or more general nonlocality, is essential.

Hence cross fertilization between continuum and discrete methods is only possible if the issue of nonlocality is clearly understood in both methods. DCM is inherently a real space method, being definitely advantageous in the study of average or local field effects. The two continuum methods we have used in the comparison, transform any nonlocal interaction into reciprocal space and store nonlocal effects in the dielectric matrix $\varepsilon(\mathbf{q}+\mathbf{G},\mathbf{q}+\mathbf{G}';\omega)$ [27]. This reciprocal space character of the continuum methods and the discrete nature of DCM prevents a direct comparison between the two strategies as to the important point of nonlocality and blocks a straightforward merging of DCM and GW (or the related Bethe–Salpeter method).

6. Summary and conclusions

To describe a condensed matter system by means of discrete dipoles in the one atom one dipole assignment, requires introduction of cells containing single atoms. When the electronic wave function cannot be confined to separate cells only (e.g. for semiconductors), cells will also influence each other directly quantum mechanically. This quantum induction requires the introduction of nonlocal polarizabilities in the discrete dipole description. A discrete dipole approach where such nonlocal polarizabilities are taken into account is called discrete cellular. The solution of the electromagnetic part of this method has been given in this paper for clusters, crystalline slabs and infinite and semi-infinite crystalline systems. The final description for the crystalline systems comes close to the double cell description derived by us before for the older discrete dipole model, using local polarizabilities only. The nonlocal polarizabilities themselves cannot be obtained in a simple manner. They require a full quantum mechanical derivation and calculation and will, therefore, be published separately. A preliminary account of it can be found already in Ref. [15]. This paper has shown that the inclusion of nonlocal polarizabilities is technically feasible and is only slightly more demanding than an equivalent discrete dipole calculation as far as the electromagnetic part of the method is concerned. We have shown that the discrete cellular method (DCM) improves significantly the quantitative aspects of RA in case of GaAs (1 1 0). The crucial difference between the traditional discrete dipole method and current DCM is in the nonlocality. Discrete dipole methods account for only one kind of nonlocality: electric. DCMs employ two kinds of nonlocality: electric and quantum mechanical.

References

[1] M. Born, E. Wolf, Principles of Optics, Pergamon Press, New York, 1980.
[2] P.P. Ewald, On the foundations of crystal optics, AFCRL-70-0580, Airforce Cambridge Research Laboratories, Translations, No. 4, 1970.
[3] P.P. Ewald, Annalen der Physik 49 (1916) 117.
[4] J. Vlieger, Physica 64 (1973) 63.
[5] O. Litzman, P. Rózsa, Surf. Sci. 66 (1977) 542.
[6] O. Litzman, Opt. Acta 25 (1978) 509.
[7] O. Litzman, Opt. Acta 27 (1980) 231.
[8] O. Litzman, Opt. Acta 29 (1982) 1317.
[9] O. Litzman, P. Mikulik, P. Dub, J. Phys. Condens. Matter 8 (1996) 4709.

[10] G.P.M. Poppe, C.M.J. Wijers, A. van Silfhout, Phys. Rev. B 44 (1991) 7917.
[11] C.M.J. Wijers, G.P.M. Poppe, Phys. Rev. B 46 (1992) 7605.
[12] C.M.J. Wijers, R. Del Sole, F. Manghi, Phys. Rev. B 44 (1991) 1825.
[13] R.G. Barrera, Proceedings of the International Workshop on Electrodynamics of Interfaces and Composite Systems, Taxco, Mexico World Scientific, Singapore, 1987.
[14] P.L. de Boeij, C.M.J. Wijers, to be published.
[15] P.L. de Boeij, Thesis, Twente University, 1997, URL: http://www.ub.utwente.nl/webdocs/tn/1/t0000013.pdf.
[16] W.K.H. Panofsky, M. Phillips, Classical Electricity and Magnetism, Addison-Wesley, Reading, MA, 1975.
[17] W.L. Mochán, R.G. Barrera, Phys. Rev. Lett. 55 (1985) 1192.
[18] P.L. de Boeij, C.M.J. Wijers, Phys. Lett. A 272 (2000) 264.
[19] G.P.M. Poppe, C.M.J. Wijers, Physica B 167 (1990) 221.
[20] P.Y. Yu, M. Cardona, Solid State Commun. 9 (1971) 1421.
[21] V. M. Agranovich, V.L. Ginzburg, Spatial Dispersion in Crystal Optics and the Theory of Excitons, Wiley, New York, 1966.
[22] N. Esser, R. Hunger, J. Rumberg, W. Richter, R. Del Sole, A. Shkrebtii, Surf. Sci. 307–309 (1994) 1045.
[23] O. Pulci, G. Onida, R. Del Sole, A.L. Reining, Phys. Rev. Lett. 81 (1998) 5374.
[24] F. Aryasetiawan, O. Gunnarson, Rep. Prog. Phys. 61 (1998) 237.
[25] G. te Velde, E.J. Baerends, Phys. Rev. B 44 (1991) 7888.
[26] G. te Velde, E.J. Baerends, J. Comput. Phys. 99 (1992) 84.
[27] W. Hanke, Adv. Phys. 27 (1978) 287.